Supplementary Information

GPR97-mediated PAR2 transactivation via a mPR3-associated macromolecular complex induces inflammatory activation of human neutrophils

Chu et al. 2022

Supplementary Table 1 Antibody list

Antibody	Antibody #Catalog	Clone	Assay
anti-CD11b	BD Biosciences #555388	ICRF44	FACS
anti-CD62L	BD Biosciences #555544	DREG-56	FACS
anti-CD11a	BD Biosciences #555379	G43-25B	FACS
anti-CD16	BD Biosciences #555407	3G8	FACS
anti-CD44	BD Biosciences #555478	G44-26	FACS
anti-CD54	BD Biosciences #559771	HA58	FACS
anti-CXCR1	BD Biosciences #555939	5A12	FACS
anti-CXCR4	BD Biosciences # 555974	12G5	FACS
anti-CD51	BD Biosciences #565835	NKI-M9	FACS
anti-CD18	BD Biosciences #555924	6.7	FACS
anti-CD18	BioLegend #302108	TS1/18	FACS
anti-CD41/CD61	BioLegend #359810	A2A9/6	FACS
anti-CD62P	BioLegend #304906	AK4	FACS
anti-CD63	BD Biosciences #557288	H5C6	FACS
anti-CD66b	BD Biosciences #561645	G10F5	FACS
anti-CD177	BioLegend #315802	MEM-166	Functional assay
anti-CD177	BioLegend #315806	MEM-166	FACS, Confocol
anti-CD177	Santa Cruz sc-376329	C5	Western blot, PLA, Functional assay
anti-Thrombin R	Santa Cruz sc-13503	ATAP2	FACS
anti-CD32	Gene Tex GTX-14572	IV.3	Functional assay
anti-PR3	Thermo Fisher MA-11945	MCPR3-2	Western blot, FACS, Confocol, Functional assay, ELISA
anti-PR3	Sanquin	CLB-12.8	FACS, Confocol, Functional assay
anti-PR3	EURO DIAGNOSTICA	4A5	Functional assay
anti-OLFM4	abcam ab85046	Polyclonal	FACS
anti-PAR2	Santa Cruz sc-13504	SAM11	Western blot, FACS, PLA, Functional assay
anti-PAR2	R&D MAB3949	#344222	Functional assay
anti-PAR2	R&D FAB3949P	#344222	FACS
normal mouse IgG_1-APC	Santa Cruz sc-2888		FACS
normal mouse IgG_1-PE	Santa Cruz sc-2866		FACS
FITC-conjugated AffiniPure Goat Anti-Rabbit IgG(H+L)	Jackson ImmunnoResearch #111-095-144	Polyclonal	FACS, Confocol
Alexa Fluor 647-conjugated goat anti-mouse IgG	Thermo Fisher A-21235	Polyclonal	FACS, Confocol
anti-EPCR	Santa Cruz sc-53982	RCR-49	FACS
anti-CD55	Santa Cruz sc-59092	BRIC 216	Western blot, FACS, Functional assay
anti-CD16	BioLegend #302002	3G8	Western blot, PLA
anti-CD62E	BD Biosciences #551144	68-5H11	FACS
anti-VCAM-1	BD Biosciences #561679	51-10C9	FACS
anti-EMR2	Invitrogen #MA5-16474	2A1	FACS, Functional assay
anti-GPR97	in house	G97-A	FACS, Western blot, PLA, Confocol, Functional assay
anti-GPR97	in house	BGP	Functional assay

Supplementary Table 2 Cell line list

Cell line	Source	Catalogue no.
HT1080	ATCC*	CCL-121™
NIH/3T3	ATCC	CRL-1658™
HeLa	ATCC	CCL-2™
M059K	ATCC	CRL-2365™
U-87 MG	ATCC	HTB-14™
C32	ATCC	CRL-1585™
COS-7	ATCC	CRL-1651™
MCF-7	ATCC	CRL-3435™
HEK-293T	ATCC	CRL-3216™
K-562	ATCC	CCL-243™
G5T/VGH	BCRC*	60194
A2058	ATCC	CRL-11147™
A375	ATCC	CRL-1619™
Jurkat	ATCC	TIB-152™
CHO-K1	ATCC	CCL-61™
MeWo	ATCC	HTB-65™
MEL-14	ATCC	HB-132™
THP-1	ATCC	TIB-202™
U-937	ATCC	CRL-1593.2™
Chang Liver	ATCC	CCL-13™
Hep-3B	ATCC	HB-8064™
Hep-G2	ATCC	HB-8065™
SK-Hep	ATCC	HTB-52™
SK-MEL5	ATCC	HTB-70™
RPMI-7951	ATCC	HTB-66™
HL-60	ATCC	CCL-240™
Raw264.7	ATCC	TIB-71™
HUVEC	BCRC	H-UV001

*ATCC: American Type Culture Collection

*BCRC: Bioresource Collection and Research Center

Supplementary Table 3 Primer list

mFc-fusion protein	Primer	Sequence (5' → 3')	Enzyme
GPR56-mFc	Forward	AATAAGCTTACAGGTGGTGACTTCCAAGAGT	HinDIII
	Reverse	AAGCGGCCGCCACCTCCACCGAGGAGACCA	NotI
CD177-mFc	Forward	AGTCCAGTGTGGTGGAATTC	EcoRI
	Reverse	AAAGCGGCCGCCTGAGAGGCAGGAGGCTGC	NotI
GPR97-mFc	Forward	ATGAATTCTTAAGCTTGGTACTCAATTCGAAGG	EcoRI
	Reverse	TAGCGGCCGCGCGTGTGAGGATATGCACCGT	NotI
$GPR56^{PLL}$/$GPR97^{GAIN}$-mFc	Forward (GPR56)	T7 primer: TAATACGACTCACTATAGGG	
	Reverse (GPR56)	GTCCACCGAGGCATTGTGAG	
	Forward (GPR97)	CACACGGCCGCTCACAATGCCTCGGTGGACAATGTGGAAAACTTGCAGAG	
	Reverse (GPR97)	CATTTGTGACACTCCTTGCAT for mFc sequence	
$GPR97^{NTD}$/$GPR56^{GAIN}$-mFc	Forward (GPR97)	T7 primer: TAATACGACTCACTATAGGG	
	Reverse (GPR97)	GTGAGCGGCCGTGTGGGGAGGACTGTGGAAGCAGGAGTCGCTGCCCGACT	
	Forward (GPR56)	TTCCACAGTCCTCCCCACAC	
	Reverse (GPR56)	CATTTGTGACACTCCTTGCAT for mFc sequence	
$GPR97^{NTD}$-mFc	Forward	T7 primer: TAATACGACTCACTATAGGG	
	Reverse	AAGCGGCCGCATTGCAGGAGTCGCTGCCCG	NotI
$GPR97^{NTD-A}$-mFc	Forward	T7 primer: TAATACGACTCACTATAGGG	
	R-primer	AAGCGGCCGCTTCCTTCATCAGATGGGCCT	NotI
$GPR97^{GAIN}$-mFc	Forward	AATGTGGAAAACTTGCAGAGATACTGGCTAAACTACGAGG	
	R-primer	CTCTGCAAGTTTTCCACATTCTGACCTGAGGTCGGGAGCA	

Supplementary Table 4 Crystallographic statistics of GPR97-ECR

DATA COLLECTION	
Source	ID30B (ESRF)
Wavelength λ (Å)	0.97625
No. of crystals	1
Resolution (Å)	96.28-3.37 (3.64-3.37)
Space group	P $4_3 2_1 2$
Cell dimensions a, b, c (Å); α, β, γ (˚)	96.3, 96.3, 172.4 90, 90, 90
Unique reflections	12030 (2398)
Multiplicity	11.6 (12.2)
Completeness (%)	99.7 (99.4)
Wilson B ($Å^2$)	103.06
R_{merge} (%)	27.3 (123.8)
R_{meas} (%)	28.6 (129.2)
R_{pim} (%)	8.3 (36.4)
$CC_{1/2}$ (%)	99.6 (52.1)
Average I/σ(I)	6.5 (1.9)

Values in parenthesis are for the highest resolution shell

REFINEMENT	
Resolution (Å)	84.11-3.37
Reflections (Work / Free set)	10967 / 1040
R_{work} / R_{free} (%)	26.59 / 31.30
No. of atoms (protein)	3640
Mean B value ($Å^2$) (protein)	134.5
R.m.s.d. bonds (Å)	0.005
R.m.s.d. angles (˚)	1.229
Ramachandran	
Favoured (%)	94.3
Allowed (%)	5.7
Outliers (%)	0.00
Molprobity score / percentile	2.03

R_{merge}: merging R-factor

R_{meas}: multiplicity-corrected merging R-factor

R_{pim}: precision-indicating merging R-factor

$CC_{1/2}$: correlation coefficients between random half data sets

R.m.s.d.: root mean square deviation from ideal geometry

Supplementary Fig. 1

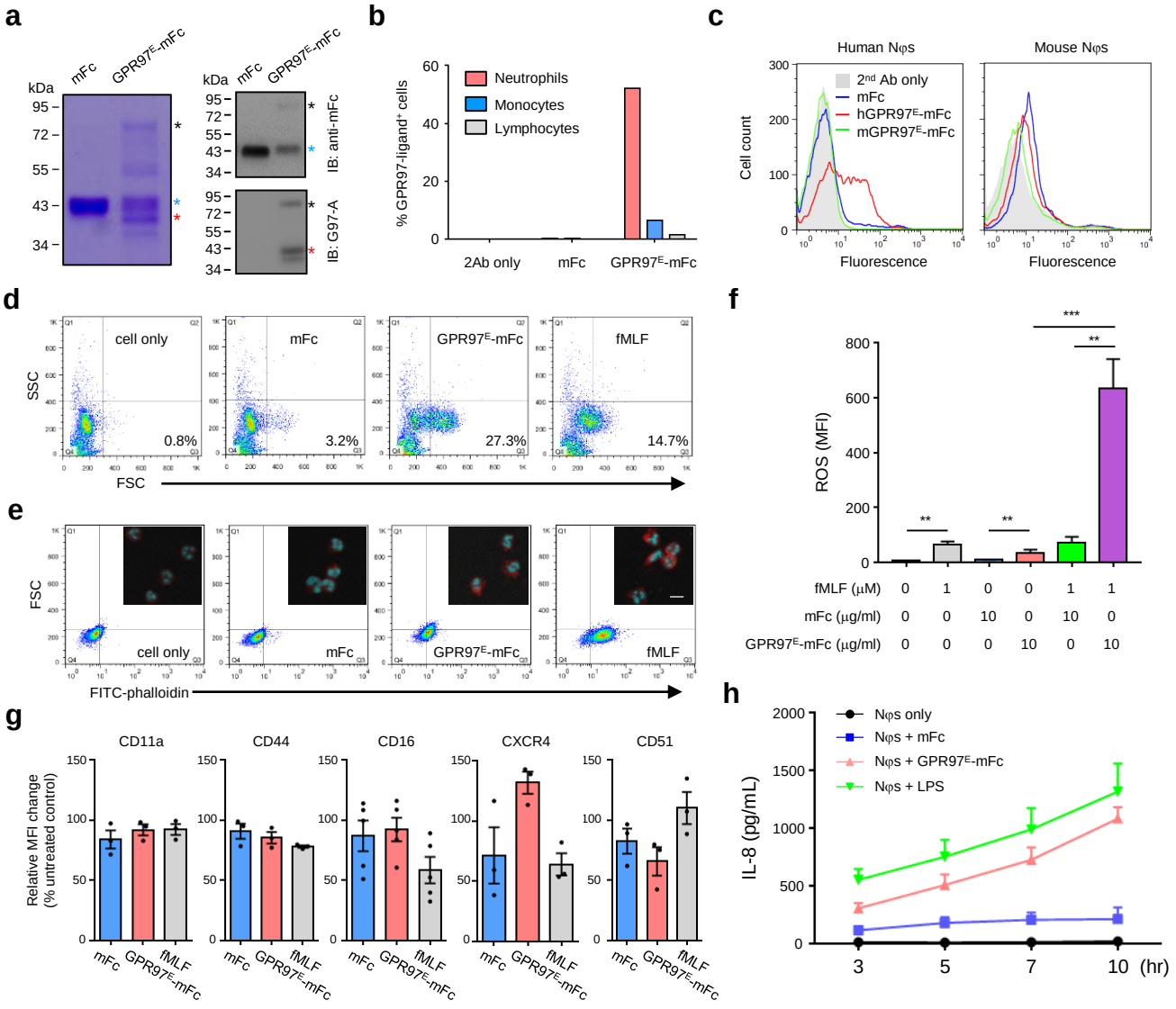

Supplementary Fig. 1 GPR97^{E}-mFc induces Nφ activation by interacting with a putative GPR97-ligand expressed in a distinct human Nφ subpopulation. **a.** Biochemical analyses of GPR97^{E}-mFc protein by coomassie blue staining in SDS-PAGE gels (left panel) and by western blotting (right panels). Left panel: the molecular weight of GPR97-NTF is ~40 kDa (indicated by red asterisk), similar to the size of mFc (blue asterisk). A minor fraction of ~82 kDa un-cleaved GPR97^{E}-mFc (black asterisk) was also expressed. The mFc-only protein was included as a control. Right panels: Western blot analyses of GPR97^{E}-mFc using Abs specific to mFc (top) and to GPR97-ECR (G97-A mAb)(bottom), respectively. **b.** Flow cytometry analyses of GPR97-ligand^{+} cells in different blood cell populations as indicated. **c.** Human Nφ-specific feature of the GPR97-ligand interaction. FACS-based ligand-binding assays were performed in purified human and mouse Nφs using human and mouse GPR97^{E}-mFc probes as indicated. **d, e.** Morphological changes of Nφs induced by GPR97^{E}-mFc were detected by flow cytometry analyses either shown as FSC/SSC plots (**d**) or FSC/F-actin staining (**e**). Photos within (**e**) were fluorescence images of cells stained with FITC-phalloidin. **f, g.** FACS analyses of ROS production (**f**) and expression of defined CD markers (**g**) in Nφs treated as indicated. **h.** Time-dependent IL-8 production of Nφs treated as indicated. Data in **f** are presented as means ± SEM of 3 independent experiments performed in triplicate and analyzed by one-way ANOVA. **p < 0.01; ***p < 0.001.

Supplementary Fig. 2

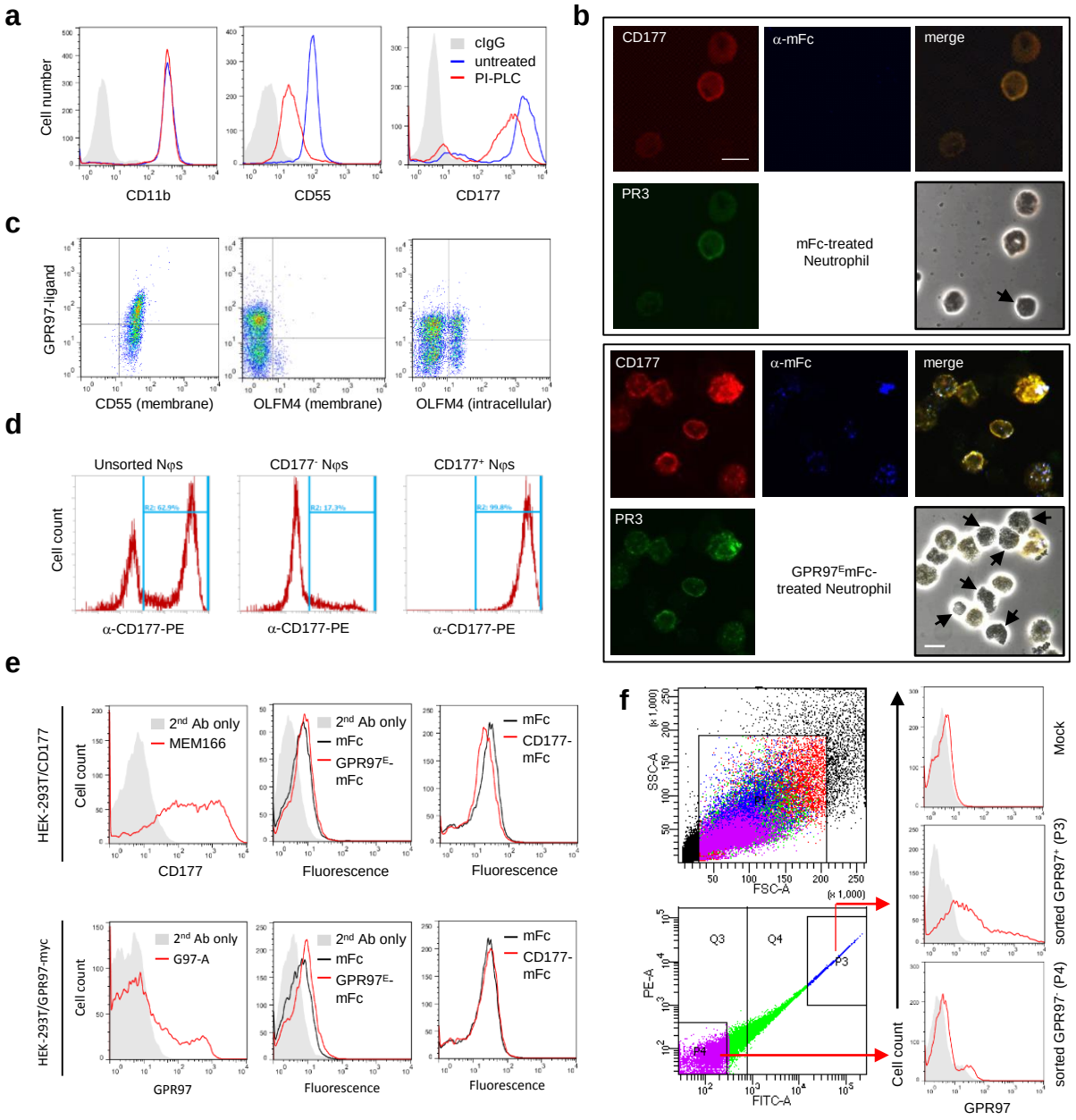

Supplementary Fig. 2 Identification of mPR3 as the GPR97-specific binding partner on human Nφs. **a.** Flow cytometry analyses of specific surface markers in Nφs treated without or with PI-PLC. Markers included CD11b, CD55, and CD177. Both CD55 and CD177 are GPI-anchored proteins while CD11b is a TM protein. **b.** Fluorescence staining of mPR3 (green) and CD177 (red) in Nφs treated with mFc or $GPR97^{E}$-mFc. The mFc-fusion protein probes were detected using anti-mFc mAb (blue). Arrows indicated $CD177^{-}$ Nφs. Scale bar, 20 μm. **c.** Dot-plots of flow cytometry analyses of Nφs double-stained with $GPR97^{E}$-mFc and anti-CD55 or anti-OLFM4. Nφs were fixed without or with membrane permeabilization to stain for membrane or intracellular proteins, respectively. **d.** Flow cytometry analyses of CD177 expression of Nφs that were subjected to MACS sorting for the enrichment of $CD177^{+}$ and $CD177^{-}$ sub-populations. **e.** Ligand-binding assays showing no homotyic and heterotypic protein-protein interactions between GPR97 and CD177. HEK-293T transfectants expressing CD177 or GPR97 were incubated with $GPR97^{E}$-mFc or CD177-mFc proteins, washed, and stained with anti-mFc mAb followed by detection with the fluorescence-labeled 2^{nd} Ab. GPR97 and CD177 expression in transfected cells were confirmed using anti-GPR97 (G97-A) and anti-CD177 (MEM166) mAbs, respectively. **f.** Flow cytometry plots showing the FACS-sorted $GPR97^{high}$ and $GPR97^{low}$ populations of HEK-293T transfectants.

Supplementary Fig. 3

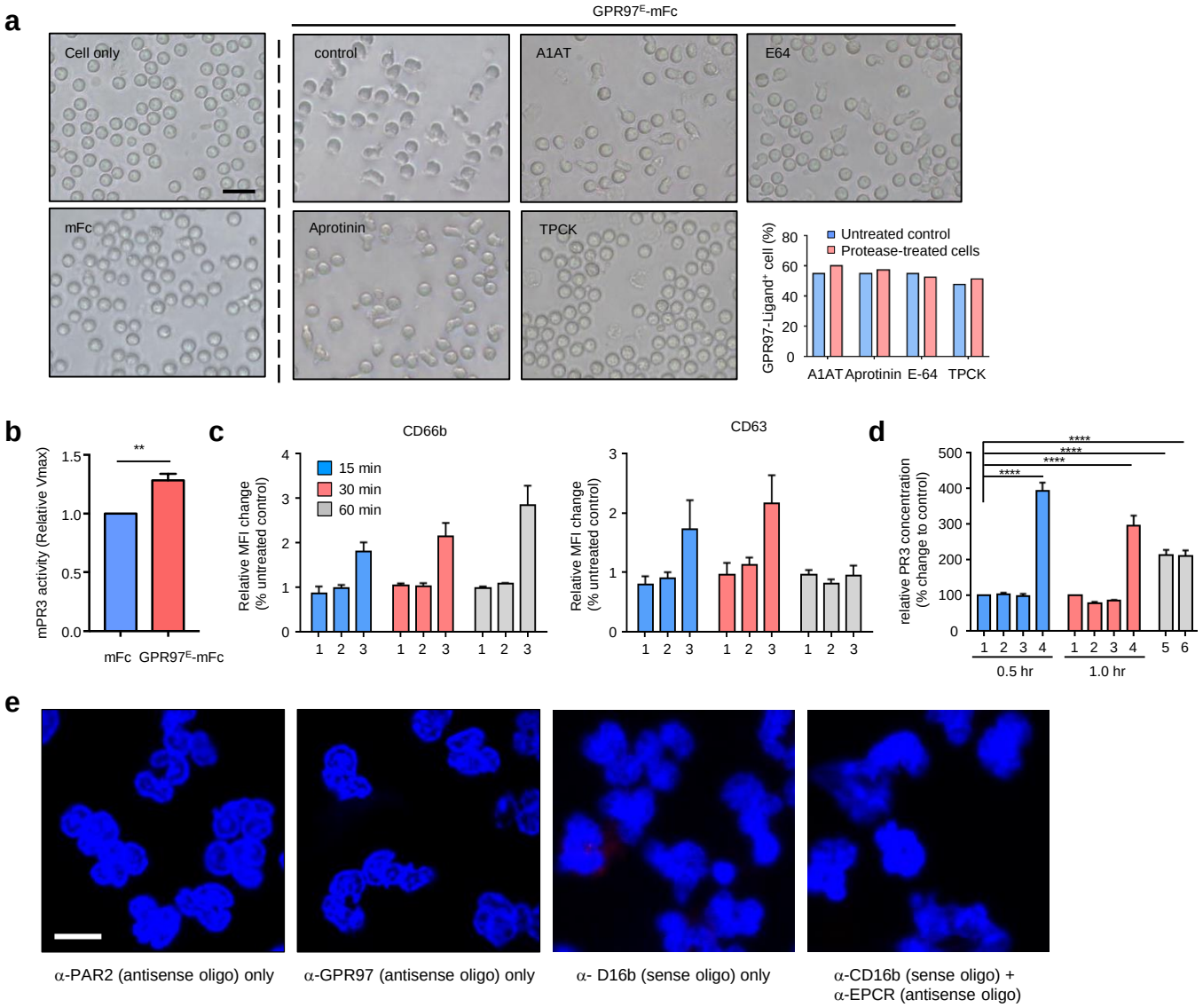

Supplementary Fig. 3 GPR97 is a positive allosteric effector of Nφ mPR3. **a.** Morphological changes of Nφs treated with GPR97^{E}-mFc in the absence or presence of protease inhibitors as indicated. Cells only and mFc-treated cells were negative controls. Scale bar, 50 μm. The lower panel at right indicated similar percentages of GPR97-ligand^{+} Nφs in the absence or presence of protease inhibitors as indicated. **b.** The relative Vmax of mPR3 enzymatic activity of Nφs incubated with mFc and GPR97^{E}-mFc. Data are presented as means ± SEM of 3 independent experiments and analyzed by unpaired student's t-test. **p < 0.01. **c, d.** Flow cytometry (**c**) and ELISA (**d**) analyses showing that GPR97^{E}-mFc treatment did not induce significant Nφ degranulation. **c.** Relative cell surface CD66b and CD63 expression levels of Nφs treated with mFc (# 1), GPR97^{E}-mFc (# 2), or fMLF (#3) for different time periods were compared with those of untreated cells. CD66b and CD63 were used as degranulation markers of specific and azurophilc granules, respectively. **d.** Relative PR3 concentration changes detected by ELISA analysis of supernatants of Nφs treated without (# 1) or with mFc (# 2), GPR97^{E}-mFc (# 3), or cytochalasin B + fMLF (# 4) for different time periods as indicated. Cells treated with A23187 (1 μM) for 10 min (# 5) and 15 min (# 6) were included as positive controls. Data are presented as means ± SEM of 3 independent experiments performed in triplicate and analyzed by one-way ANOVA. ****p < 0.0001. **e.** Results of the PLA analyses showing the minimal background signals when using mAb probes for single receptors and non-associated receptor pairs as indicated. Scale bar, 10 μm.

Supplementary Fig. 4

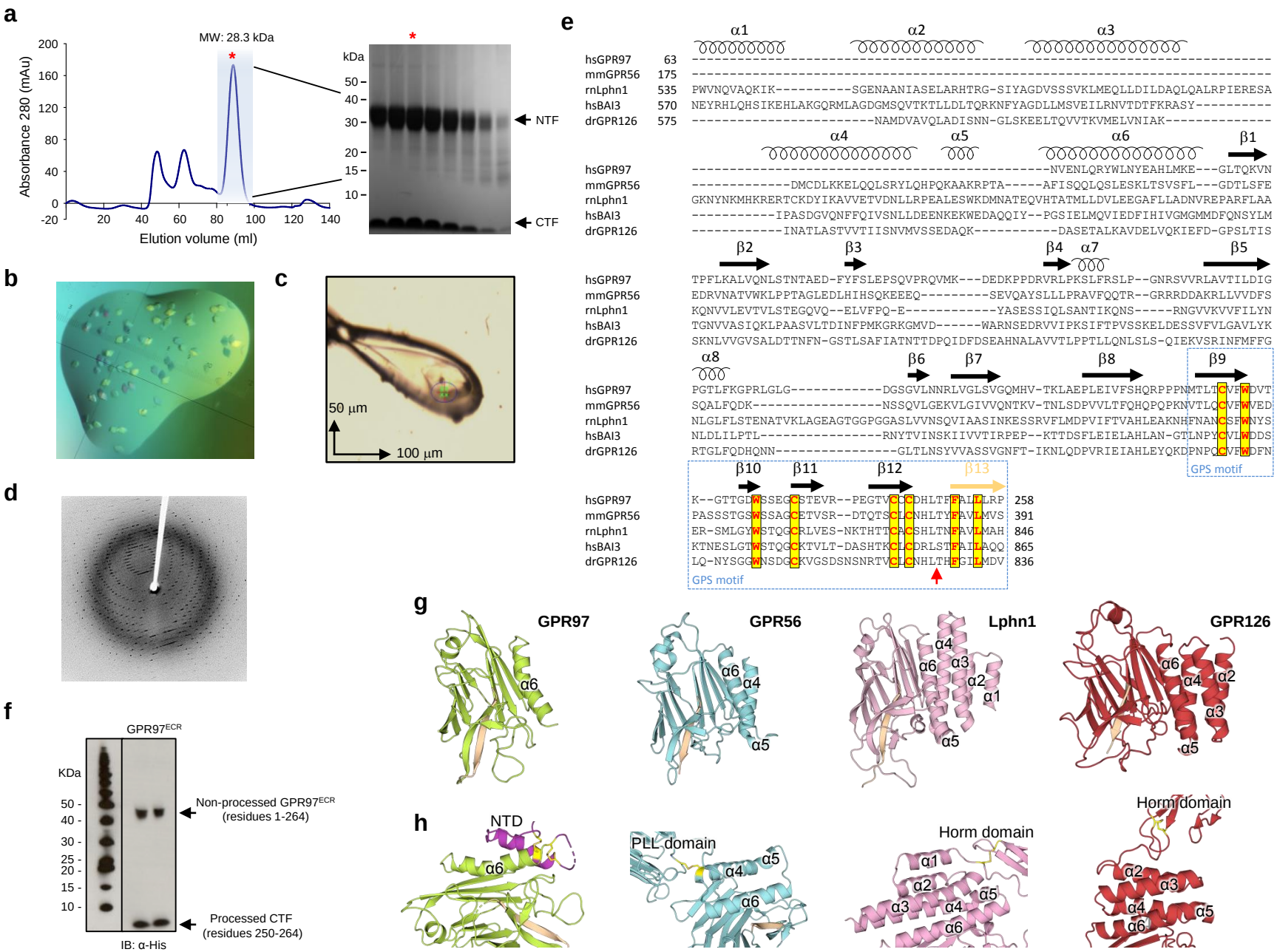

Supplementary Fig. 4 Crystallographic studies of GPR97^{ECR}. **a.** Representative SEC elution profile and SDS-PAGE analysis of purified GPR97^{ECR} purification. The red asterisk indicated the GPR97^{ECR}-containing SEC peak and protein purity was assessed by coomassie blue staining in SDS-PAGE gels. GPR97^{ECR} run as two bands (NTF and CTF) on the SDS-PAGE gel due to autoproteolysis of its GAIN domain. **b.** GPR97^{ECR} crystals were grown in 1.8 M tri-ammonium citrate pH 7. **c.** Crystals were cryo-protected and individually assessed for diffraction quality. **d.** A representative image from the native X-ray diffraction dataset collected at the ESRF beamline ID30B. **e.** Sequence alignment of the GAIN domain of *Homo sapiens* GPR97 with those crystallised and available in the PDB database: *Mouse musculus* GPR56, *Rat norvegicus* Lphn1, *Homo sapiens* BAI3 and *Danio rerio* GPR126. The secondary structure was displayed on top of the sequence. The GPS motif is indicated by the blue box and the GPS site is indicated by a red arrow. Residues highly conserved in the GAIN domains of all aGPCRs are highlighted in yellow and shown in bold red. **f.** Western blotting using α-His mAb to detect the C-terminal His_6-tail fused to GPR97^{ECR}. The presence of two bands indicated GPR97^{ECR} exists as a mixture of autoproteolysed and non-cleaved species. **g.** Structural comparison of GPR97 GAIN domain with those crystallised and available in the PDB database (PDB IDs: 5KVM (GPR56), 4DLQ (Lphn1), 6V55 (GPR126)). **h.** Close-up of the interdomain disulphide bridges linking the GAIN domain of GPR97, GPR56, Lphn1 and GPR126 to the NTD, PLL domain, Horm domain and Horm domain, respectively.

Supplementary Fig. 5

a

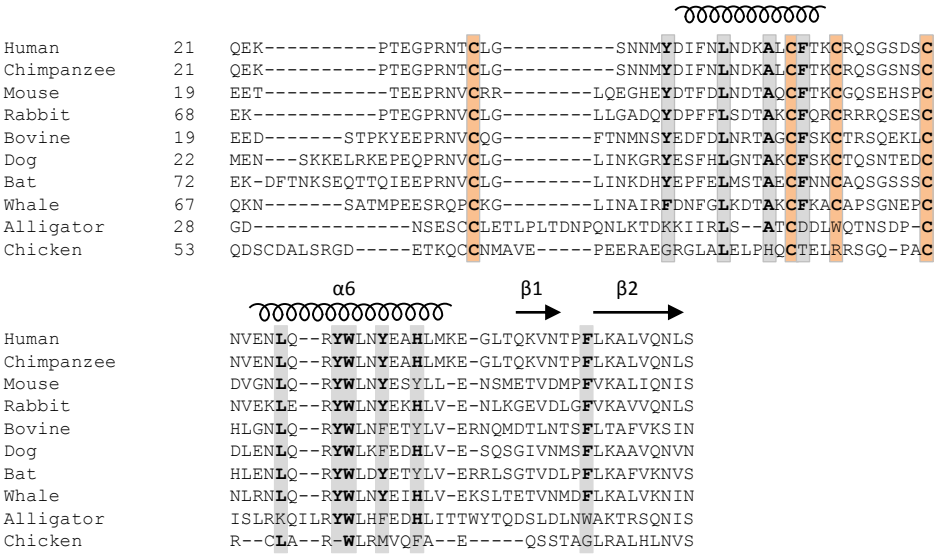

b

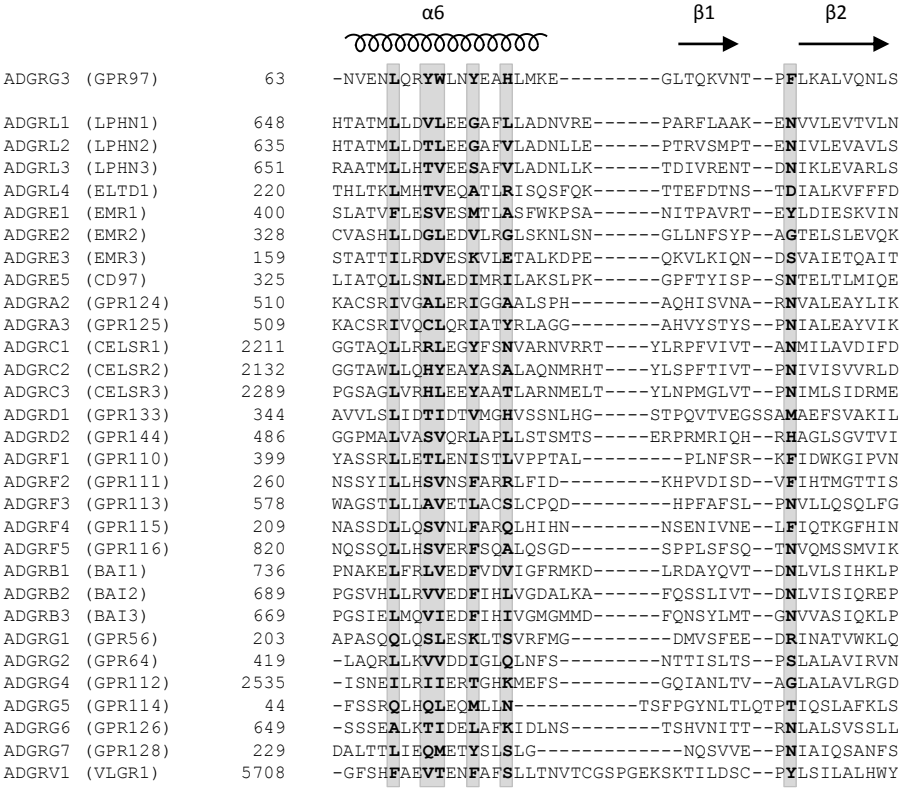

Supplementary Fig. 5 The NTD is stabilised by hydrophobic interactions conserved in all GPR97 orthologs, but not found in other GAIN domains. **a.** Sequence alignment with secondary structure of the NTD, α6 helix and β1-β2 strands of the GAIN domain of GPR97 orthologs. The conserved cysteines involved in known disulphides bridges are shown in bold and highlighted in yellow. The conserved residues involved in the hydrophobic interactions stabilising the NTD to the GAIN domain are shown in bold and highlighted in grey. **b.** Sequence alignment with secondary structure of the α6 helix and β1-β2 strands of the GAIN domain of all aGPCRs. The residues involved in stabilising GPR97 NTD to its GAIN domain are shown in bold and highlighted in grey.

Supplementary Fig. 6

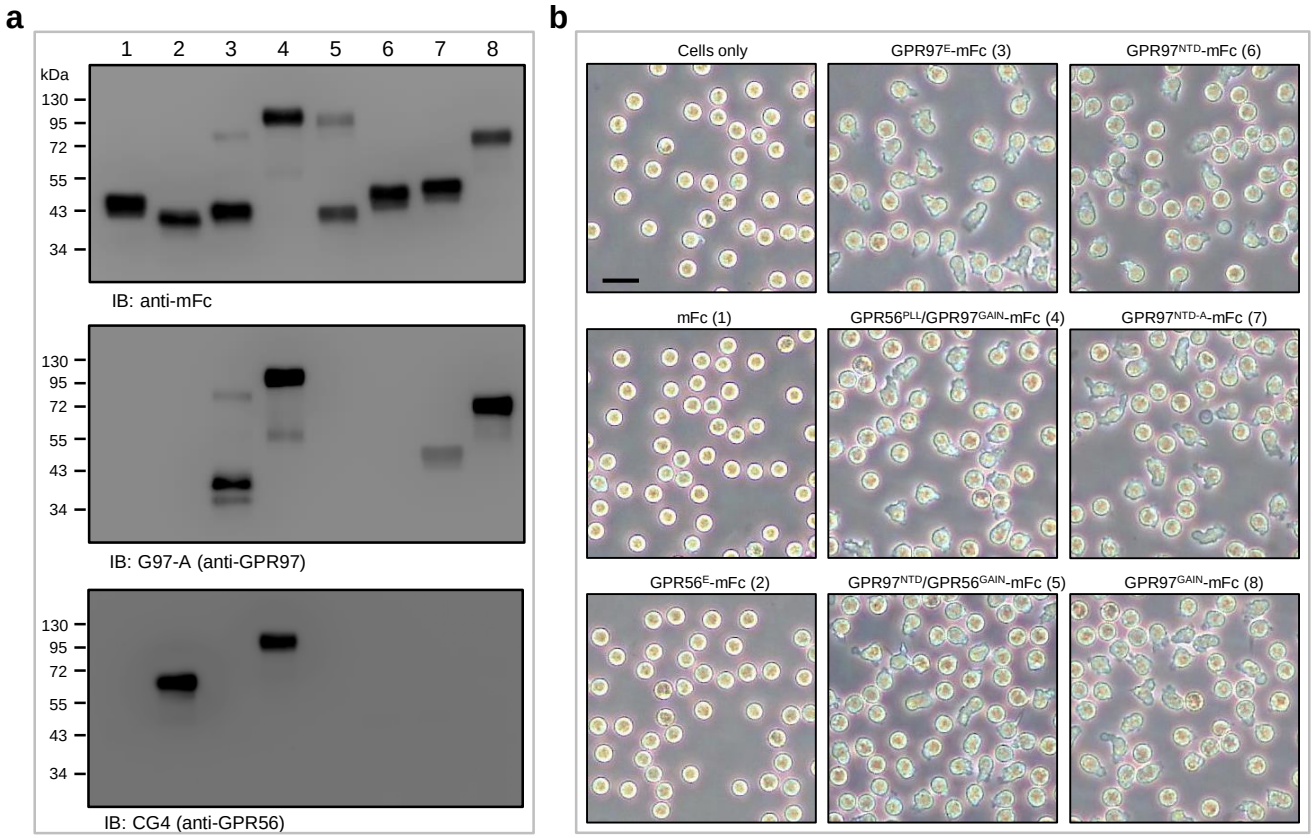

Supplementary Fig. 6 Mapping of the mPR3-binding regions in GPR97-ECR. **a.** Western blot analyses of the domain-swapped and domain-truncated $GPR97^{E}$-mFc probes. Lane 1, mFc only; 2, $GPR56^{E}$-mFc; 3, $GPR97^{E}$-mFc; 4, $GPR56^{PLL}$/$GPR97^{GAIN}$-mFc; 5, $GPR97^{NTD}$/$GPR56^{GAIN}$-mFc; 6, $GPR97^{NTD}$-mFc; 7, $GPR97^{NTD\text{-}A}$-mFc; 8, $GPR97^{GAIN}$-mFc. Blots were probed with anti-mFc (top panel), G97-A (anti-GPR97 mAb)(middle panel), and CG4 (anti-GPR56 mAb)(lower panel), respectively. **b.** Morphological changes of Nφs induced by various $GPR97^{E}$-mFc probes as indicated. Cells only and those treated with mFc and $GPR56^{E}$-mFc were included as negative controls. Scale bar, 50 μm.

Supplementary Fig. 7

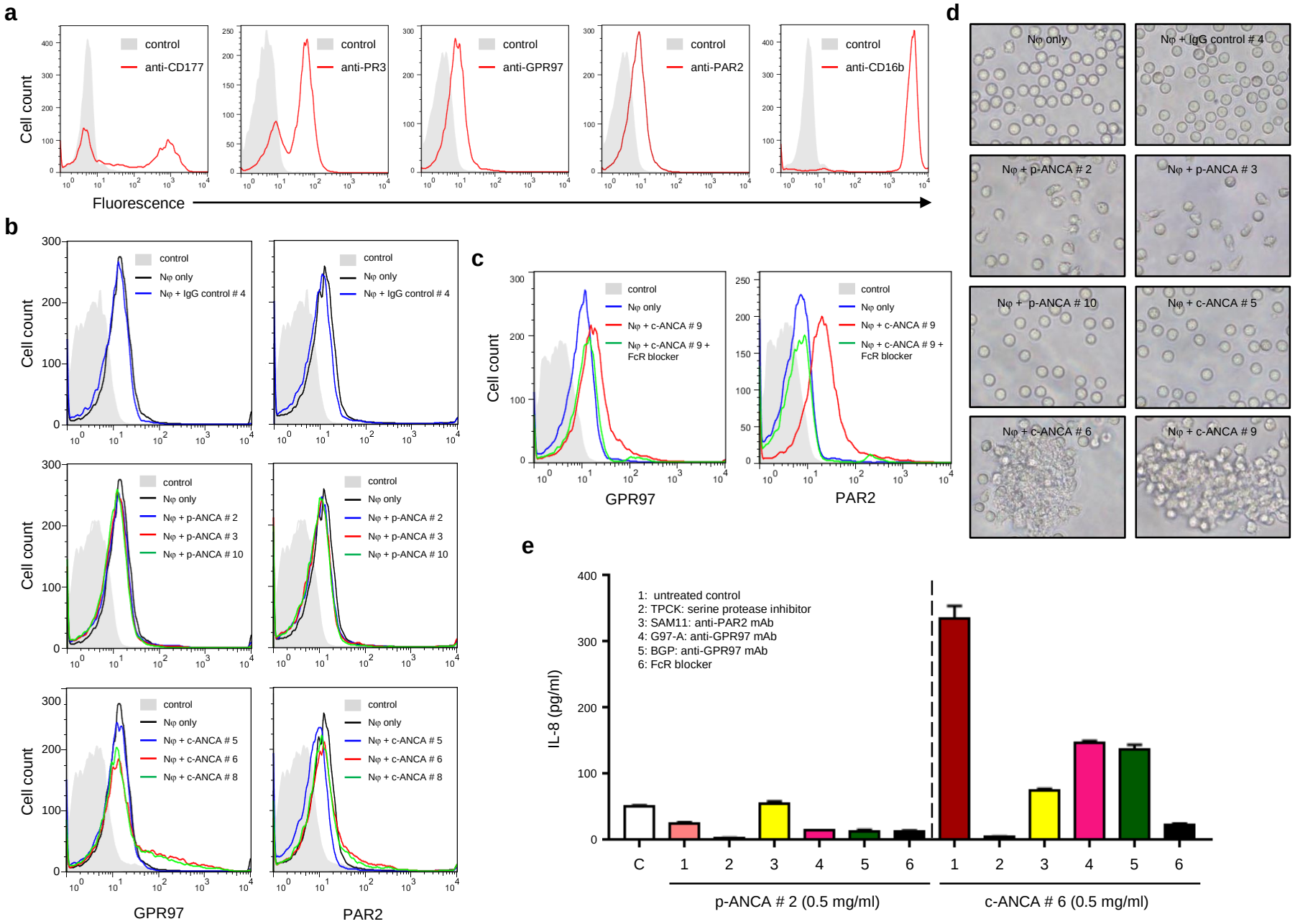

Supplementary Fig. 7 Expressional regulation of GPR97 and PAR2 in Nφs. **a.** Representative expression profiles of indicated receptors in resting human Nφs detected by flow cytometry. **b.** Flow cytometry analysis of up-regulated GPR97 and PAR2 expression in Nφs incubated with purified PR3-ANCA IgGs but not purified MPO-ANCA IgGs as indicated. **c.** Representative flow cytometry analyses of FcR-dependent GPR97 and PAR2 up-regulated expression in Nφs incubated with purified PR3-ANCA IgGs. **d.** Representative light microscope images showing aggregates of Nφ incubated with purified PR3-ANCA IgGs but not purified MPO-ANCA IgGs as indicated. Nφs only and those treated with control IgGs from a normal subject were included as negative control. **e.** ELISA analyses of IL-8 secreted by Nφs incubated with purified PR3-ANCA or MPO-ANCA IgGs in the absence or presence of protease inhibitors or blocking reagents as indicated. Data shown were results of one representative experiment done in triplicate.